

# Feedback Effects in Plasmonic Slot Waveguides Examined Using a Closed Form Model

Mohamed A. Swillam, *Senior Member, IEEE*, and Amr S. Helmy, *Senior Member, IEEE*

**Abstract**—Analysis of the feedback effects in plasmonic waveguides is carried out using an analytical model. The closed-form model is extracted from the waveguide physical parameters is simple, accurate, and provides insight into understanding the feedback effects in plasmonic waveguide structures. These feedback effects are utilized to obtain various filter functions using the same base structures, with exceptional tolerance to fabrication imperfections in comparison to its plasmonic and dielectric counterparts.

**Index Terms**—Nanophotonics, nanoresonators, optical circuits, optical filter, plasmonics.

## I. INTRODUCTION

NANOPHOTONICS empowered by nanoscale plasmonic waveguides (NPWs), have recently been exploited in a wide range of application domains. This is due to their ability to confine and manipulate light on the nanoscale. Their nanoscale confinement and versatility enhances numerous applications, especially in the fields of sensing and biomedical diagnostics [1],[2]. NPWs also provide an attractive platform for on-chip optical interconnects. In particular, plasmonic slot waveguides (PSW), which have the potential to replace the electrical interconnect buses in integrated circuits due to their beneficial characteristics. Challenges such as propagation losses and efficient in-coupling hindered the exploitation of these devices. Recently, the coupling bottleneck has been resolved by designing efficient wideband non-resonant couplers between PSWs and dielectric waveguides [3].

The aforementioned applications are wavelength selective and require some wavelength filtering functions. Various designs to implement filter functions in NPWs have been presented recently [4]-[6]. However, most of these solutions are based on sharp resonances. Strong resonance-based structures pose formidable challenges in fabrication tolerances given the nanoscale dimensions associated with these designs. In addition, the design process has been hindered by the lack of suitable analytical design models to and the associated insight into the device physics.

Manuscript received July 2, 2011; revised November 21, 2011; accepted December 12, 2011. Date of publication December 22, 2011; date of current version March 2, 2012.

M. A. Swillam is with the Edward S. Rogers Sr. Department of Electrical and Computer Engineering and Institute of Optical Sciences, University of Toronto, Toronto ON M5S 1A7, Canada, and also with the Department of Physics, American University in Cairo, New Cairo 11835, Egypt (e-mail: m.swillam@aucegypt.edu).

A. S. Helmy is with the Edward S. Rogers Sr. Department of Electrical and Computer Engineering and Institute of Optical Sciences, University of Toronto, Toronto, ON M5S 1A7, Canada (e-mail: a.helmy@utoronto.ca).

Color versions of one or more of the figures in this letter are available online at <http://ieeexplore.ieee.org>.

Digital Object Identifier 10.1109/LPT.2011.2181350

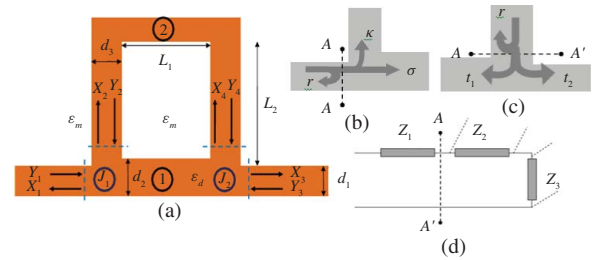


Fig. 1. (a) Schematic diagram of a scheme to control light beaming. (b)–(d) Schematic diagram of the T-junctions and its equivalent circuit model.

To date, the preferred method to model most filters is finite difference time domain (FDTD) simulations. These are numerical techniques that require intensive computation power, which requires long simulation cycles, while providing little physical insight into the design of the device in comparison to their analytical counterparts.

In this Letter, we develop closed form model to describe light propagation in plasmonic gap waveguide. The model is an equivalent network model for the straight waveguides and their junctions. The accuracy of this model has been confirmed using FDTD simulations. Unlike FDTD, this model is fast, and efficient with a complexity that does not scale with the dimensions of the structure. As a result, this model allows for the efficient design and optimization of various devices.

The model is then exploited to examine feedback effects in PSWs. Further, we use the properties of feedback branches in PSWs to realize devices with useful functionality utilizing simple structures with significant tolerance to fabrication imperfections.

## II. THEORETICAL ANALYSIS OF FEEDBACK EFFECT

Initially we develop a closed form model describing the propagation in the feedback network shown in Fig.1 and analyze its effect. In the model, the interference between the forward and the backward waves generated using the feedback path determine the response of the entire structure. The interference depends on the path length of the feedback junction and the amount of the light coupled to this junction. Thus, by controlling the feedback path dimensions, the structure can produce various filter responses. In order to analyze its performance of, the scattering matrix of the structure is defined as

$$\begin{pmatrix} X_1 \\ X_2 \\ X_3 \\ X_4 \end{pmatrix} = \begin{pmatrix} S_{11} & S_{12} & S_{13} & S_{14} \\ S_{21} & S_{22} & S_{23} & S_{24} \\ S_{31} & S_{32} & S_{33} & S_{34} \\ S_{41} & S_{42} & S_{43} & S_{44} \end{pmatrix} \begin{pmatrix} Y_1 \\ Y_2 \\ Y_3 \\ Y_4 \end{pmatrix} \quad (1)$$

This matrix can be solved to obtain the transmission from the output (right) port due to the excitation at the input (left) port as shown in Fig.1. To calculate the transmission, we assume that there is no input power from the output port,  $Y_3 = 0$ . Superposition can be applied if more than one port is excited simultaneously. The field inside the feedback path can be connect through a phase relation given as

$$Y_4 = X_2 e^{-\phi_t}, \quad \text{and} \quad Y_2 = X_4 e^{-\phi_t} \quad (2)$$

By using (1) and substitute from (2), we can write

$$X_2 = \frac{S_{21}Y_1 + S_{22}X_4 e^{-\phi_t}}{(1 - S_{24}e^{-\phi_t})} \quad \text{and,} \quad X_4 = \frac{S_{41}Y_1 + S_{44}X_2 e^{-\phi_t}}{1 - S_{42}e^{-\phi_t}} \quad (3)$$

The transmission coefficients can thus be calculated as

$$T = \frac{X_3}{Y_1} = \frac{S_{31}Y_1 + S_{32}X_4 e^{-\phi_t} + S_{34}X_2 e^{-\phi_t}}{Y_1} \quad (4)$$

By substituting (3) into (4), we get

$$\begin{aligned} T = S_{31} &+ \frac{S_{34}S_{21}e^{-\phi_t}}{1 - S_{24}e^{-\phi_t}} + \frac{S_{32}S_{41}e^{-\phi_t}}{1 - S_{42}e^{-\phi_t} - \frac{S_{44}S_{22}e^{-2\phi_t}}{1 - S_{24}e^{-\phi_t}}} \\ &+ \frac{S_{32}S_{44}S_{21}e^{-2\phi_t}}{(1 - S_{24}e^{-\phi_t})(1 - S_{42}e^{-\phi_t} - \frac{S_{44}S_{22}e^{-2\phi_t}}{1 - S_{24}e^{-\phi_t}})} \\ &+ \frac{S_{22}S_{34}S_{41}e^{-2\phi_t}}{(1 - S_{24}e^{-\phi_t})(1 - S_{42}e^{-\phi_t} - \frac{S_{44}S_{22}e^{-2\phi_t}}{1 - S_{24}e^{-\phi_t}})} \\ &+ \frac{S_{22}S_{34}S_{44}S_{21}e^{-3\phi_t}}{(1 - S_{24}e^{-\phi_t})^2(1 - S_{42}e^{-\phi_t} - \frac{S_{44}S_{22}e^{-2\phi_t}}{1 - S_{24}e^{-\phi_t}})} \end{aligned} \quad (5)$$

where  $S_{21} = -jk$ ,  $S_{24} = t_{2,1}\kappa_1 e^{-\phi_1}$ ,

$$\begin{aligned} S_{31} &= \sigma_1\sigma_2 e^{-\phi_1}, \quad S_{34} = jt_{2,2}S_{32} = jt_{1,2}\sigma_2 e^{-\phi_1}, \\ S_{42} &= t_{1,2}\kappa_2 e^{-\phi_1}, \quad \text{and} \quad S_{44} = S_{22} = -r \end{aligned} \quad (6)$$

The term  $\phi_1 = (\alpha_1 + j\beta_1)L_1$ , and  $\phi_t = (\alpha_2 + j\beta_2)(2L_2 + L_1)$  are the phases in the main path, arm 1, and the feedback path, arm 2, respectively as shown in Fig.1. As shown in (6), the effect of the propagation through arm 1 is included in the scattering terms.

The coefficients  $\tau$ ,  $\kappa$ ,  $\sigma$  and  $\rho$  are the transmission, coupling, through, and reflection coefficients for each  $T$ -junction, respectively. These coefficients are calculated at each port for both junctions as shown in Fig.1 as an example. These parameters can be estimated using the simple transmission line circuit model shown in Fig.1d. According to this model the reflection and transmission are

$$r = \left| \frac{Z_t - Z_1}{Z_t + Z_1} \right|, \quad \tau = \sqrt{\frac{Z_n}{Z_t}} \times \frac{2\sqrt{Z_1 Z_t}}{(Z_1 + Z_t)}, \quad (7)$$

where  $\tau = t$  or, or  $\sigma$ , or  $\kappa$ .  $Z_1$  is the PSW guided mode impedance at the port ( $Z_1 = \beta d/\omega e$ ), and  $Z_t$  is the total load impedance, which may contain the resultant of the guided impedance at the output waveguide. It also takes into account the loading effect of the waveguides in the adjacent junction.

A similar expression for the reflection  $R$  can be also obtained. The impedance model given in (7) has been verified using FDTD and it fits well for PSW waveguides with slot

width less than 250 nm with accuracy within 5%. For larger widths, the amount of the power coupled to the orthogonal arms is reduced and model deviates from the FDTD. This reduction is due to the changes in the nature of the fundamental mode in this waveguide, which occur for larger thicknesses.

Using this simple model, all the scattering matrix coefficients can be described using the impedance values of each of the waveguide segments in the network. These values can be obtained by calculating the propagation constant of the MIM structure. In contrast, FDTD simulations require solving for the eigenmodes of the structure to obtain the excitation profile in the waveguides. This is not the case for the model developed here. The time required to run FDTD simulations is significantly longer and does not lend itself to providing insight into device optimization. Both methods provide similar results as will be shown. Using our model, an analytical sensitivity expression can be obtained for all terms with respect to the design parameters. This expression can be easily calculated via the derivative of the response in (5) with respect to all the design parameters. This allows for determining the most critical parameters that govern the structure performance.

Using this model we investigate feedback effects in PSWs. As shown in Fig. 1.a, a typical structure is based on creating a feedback path using two  $T$ -junctions. It utilizes the ability of PSWs to efficiently couple light through sharp bends without considerable loss [5]. We will show next that using the same network can provide band pass and band reject responses with a wide range of spectral properties. This can be achieved by modifying the dimensions in the feedback branch.

This feedback structure differs from the dielectric and plasmonic ring resonator as the forward and backward waves in the feedback arm (arm 2) are connected to the main path through two junctions instead of one. Also the feedback loop shares part of its path (arm 1) with the main path which may allow for interference between the fields in both paths. These unique properties provide more degrees of freedom that enable further tailoring of the response and hence achieve more complex functionality using simple structures. Unlike any resonator based structures, these properties also afford various spectral responses and are not limited to notch response only, as shown in the following examples. The structure is also much more compact due to the utilization of the  $T$ -junctions, which allow for ultra-compact power splitting with any desired ratio between the two paths.

### III. NUMERICAL VERIFICATIONS AND APPLICATIONS

The model is used for design and optimization of a flat and wideband band pass filter of 400 nm 3dB bandwidth around the wavelength of 1550 nm as shown in Fig.2. The dimensions of the structure are  $d_1 = d_2 = 60$  nm, and  $d_3 = 100$  nm. The length and width of the feedback path  $L_1$  and  $L_2$  are 320 nm and 420 nm. In all examples, the wavelength dependence of physical parameters has been taken into account.

The results have also been confirmed by 2-D FDTD simulations by using metal-insulator-metal configuration and show good agreement as shown in Fig.3. For the FDTD

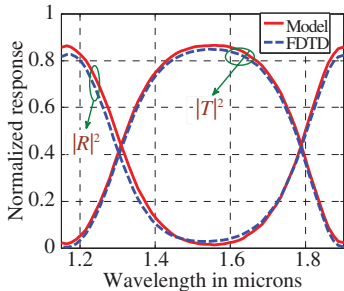


Fig. 2. Transmission of feedback structure with asymmetric junction.

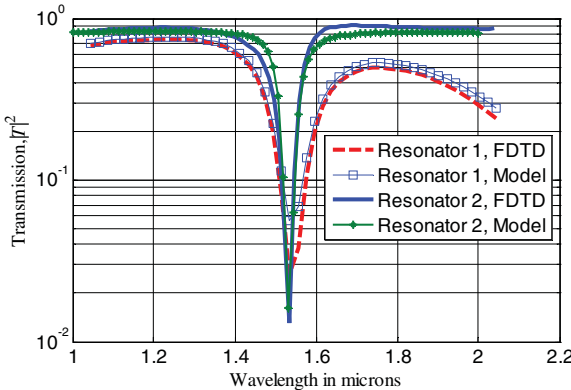


Fig. 3. Transmission characteristics of two types of resonators using feedback plasmonics scheme. The inset is the schematic diagram of resonator 2.

simulations, a spatial step is taken to be 1.0 nm in both directions. A commercial FDTD tool, Lumerical, has been exploited in these applications. It is worth noting that the computational time of our model is less than a second. However, the 2D FDTD simulation time takes up 2.5 hours for each run on the same machine. Other numerical methods such as the frequency domain approaches may be more efficient than the FDTD for single frequency calculations. However, for wideband frequency calculations they may be comparable to the FDTD. The model has been also verified in the 3D case and has very good agreement with 3-D FDTD which takes up to 8.0 hours of simulation time. Thus, for the optimization processes, which require few tens of iterations, our model requires practical time in comparison to FDTD.

The feedback effect has shown significant versatility in comparison to its counterparts. Controlling the amount of the light coupled out from the feedback path can change the characteristics of the transmission response significantly. For example, in the aforementioned example, most of the light is coupled out of the feedback branch over the band of interest. Conversely, by minimizing this coupling it is possible to create a resonance effect inside the feedback branch (arm 2). Thus, by adjusting this path length such that  $L_1 + 2L_2 = m\lambda/2n_{eff}$ , the structure can operate as a resonant band-reject notch filter.

The control of the coupled light is mainly carried out by engineering the ports of the  $T$ -junctions via controlling the width of the different waveguide sections, which effectively change their impedance. This will in turn change the transmission, through, and reflection properties. For example, for designing Resonator 1, shown in Fig.3, we utilize  $d_1 = d_2 = 50$ ,  $d_2 = 30$  nm and  $L_1 = 200$  nm, and  $L_2 = 350$  nm. However, reducing the width of the slot increases the losses and degrades the performance of the resonator. To overcome this

impediment, the design has been optimized to further increase the quality factor and the extension ratio. In this optimized design; namely Resonator 2, a narrow PSW is exploited at the  $T$ -junctions only ( $d_3 = 40$  nm) to obtain the required resonant effect. Wider feedback path to reduce the losses ( $d_2 = 300$  nm) is also exploited as shown in the inset of Fig.3. The length of the junctions  $L_1$ , and  $L_2$  are optimized to be 150 nm, and 700 nm, respectively. The transmission characteristics of this modified structure are also shown in Fig. 3 with smaller loss and higher quality factor than for Resonator 1. The footprint of this resonator is only 500 nm  $\times$  700 nm. For this resonator, the quality factor reaches 78 with extinction ratio of 17.5 dB and small insertion loss  $\sim 1$  dB.

The same quality factor is obtainable with other plasmonic resonator designs. However other designs require dimensions on the same scale to those that are required for dielectric structures [7]. In contrast, the designs described here have a footprint area, which is two orders of magnitude smaller. Thus, the insertion losses associated with our structures can be made lower. This can lead to much higher extinction ratios. The length of the resonator is only  $\lambda g/2$  which is the smallest obtainable resonator dimension. Of more significance is that these resonators are less sensitive to fabrication tolerances in comparison to their dielectric counterparts. For example, a 10% change in the diameter of dielectric ring resonator causes a shift of 3% in the center wavelength at 1500 nm. The dielectric resonator is designed using SOI with radius of 1  $\mu$ m. On the other hand, the plasmonic resonators proposed here exhibits 0.3% shift at the same center wavelength. The low sensitivity of these devices may come from the compactness of the devices and also from the weak dependence of the design parameters on the wavelength [3].

#### IV. CONCLUSION

We propose an analytical model PSWs with feedback . The model is closed form, efficient and allows for rapid device optimization. The model is utilized to study a novel and simple plasmonic structure where feedback is utilized. The results agree well with results obtained from FDTD simulations. The design rules and the physical insight into the operation of this feedback structure have also been discussed in light of the insight provided from this closed form model.

#### REFERENCES

- [1] P. Berini, "Bulk and surface sensitivities of surface plasmon waveguides," *New J. Phys.*, vol. 10, p. 105010, Oct. 2008.
- [2] M. A. Swillam and A. S. Helmy, "Analysis and applications of 3-D rectangular metallic waveguides," *Opt. Express*, vol. 18, no. 19, pp. 19831–19843, 2010.
- [3] B. Lau, M. A. Swillam, and A. S. Helmy, "Hybrid orthogonal junctions: Wideband plasmonic slot-silicon waveguide couplers," *Opt. Express*, vol. 18, no. 26, pp. 27048–27059, 2010.
- [4] B. Yun, G. Hu, and Y. Cui, "Theoretical analysis of a nanoscale plasmonic filter based on a rectangular metal-insulator-metal waveguide," *J. Phys. D, Appl. Phys.*, vol. 43, no. 38, pp. 385102-1–385102-8, 2010.
- [5] A. Hosseini and Y. Massoud, "Nanoscale surface plasmon based resonator using rectangular geometry," *Appl. Phys. Lett.*, vol. 90, no. 18, pp. 181102-1–181102-3, Apr. 2007.
- [6] Z. Han, V. Van, W. N. Herman, and P.-T. Ho, "Aperture-coupled MIM plasmonic ring resonators with sub-diffraction modal volumes," *Opt. Express*, vol. 17, no. 15, pp. 12678–12684, 2009.
- [7] E. Feigenbaum and H. A. Atwater, "Resonant guided wave networks," *Phys. Rev. Lett.*, vol. 104, no. 14, pp. 147402-1–147402-4, Apr. 2010.